Comparison of MoS₂, WS₂ and Graphene Oxide for DNA Adsorption and Sensing

Chang Lu[1,2], Yibo Liu[2], Yibin Ying[1] and Juewen Liu[2*]

1. College of Biosystems Engineering and Food Science, Zhejiang University, Hangzhou

310058, China

2. Department of Chemistry, Waterloo Institute for Nanotechnology, University of Waterloo,

Waterloo, Ontario, Canada, N2L 3G1.

Email: liujw@uwaterloo.ca

Abstract

Interfacing DNA with two-dimensional (2D) materials has been intensely researched for various analytical and biomedical applications. Most of such studies were performed on graphene oxide (GO), and two metal dichalcogenides, MoS_2 and WS_2; all of them can all adsorb single-stranded DNA. However, they like use different surface forces for adsorption based on their chemical structures. In this work, fluorescently labeled DNA oligonucleotides were used and their adsorption capacity and kinetics were studied as a function of ionic strength, DNA length and sequence. Desorption of DNA from these surfaces were also measured. DNA is more easily desorbed from GO by various denaturing agents, while surfactants yield more desorption from MoS_2 and WS_2. Our results are consistent with that DNA can be adsorbed by GO via π–π stacking and hydrogen bonding, MoS_2 and WS_2 mainly use van der Waals force for adsorption. Finally, fluorescent DNA probes were adsorbed by these 2D materials for detecting the complementary DNA. For this assay, GO gave the highest sensitivity, while they all showed a similar detection limit. This study has enhanced our fundamental understanding of DNA adsorption by two important types of 2D materials and is useful for further rational optimization of their analytical and biomedical applications.

Introduction

Nanomaterials for DNA adsorption are useful for delivering therapeutic nucleic acids,[1] designing smart stimuli-responsive materials,[2, 3] and developing biosensors.[4-6] In particular, two-dimensional (2D) materials have recently emerged as a unique platform for interfacing with DNA. Compared to traditional nanoparticles, 2D materials often have a larger specific surface area. Developments in this field was stimulated by the discovery of graphene.[7] To disperse in water and interface with biopolymers, graphene oxide (GO) is often used.[8-10] The interaction between GO and DNA has been extensively studied,[11-15] which has inspired the exploration of various other 2D materials. Among them, MoS_2 and WS_2 are two representative examples.[16-19] Using these two materials for DNA-based sensing was reported with simple DNA oligonucleotides,[20-27] as well as aptamers,[28, 29] and DNAzymes.[30] Thiolated DNA was also attached to AuNPs to improve sensing based the intrinsic photoluminescence property of MoS_2.[31] Adsorption of DNA improves the colloidal stability of MoS_2 nanosheets,[32] and DNA can even exfoliate WS_2,[33] suggesting a strong interaction.

Aside from these applied research, only a few fundamental studies were reported. Theoretical work pointed out that van der Waals (vdW) force is mainly responsible for DNA base adsorption by MoS_2 and WS_2.[34, 35] A comparison was made for DNA adsorption on these materials using fluorescently labeled magnetic nanoparticle probes.[36] MoS_2, WS_2 and GO can all adsorb single-stranded (ss) DNA while repel double-stranded (ds) DNA.[37] By examining their chemical structures, one can readily see that MoS_2 and WS_2 are quite different from GO. For example, GO can adsorb DNA via pi-pi stacking with DNA bases, while MoS_2 and WS_2 are non-aromatic.

Given the increasing importance of these 2D dichalcogenide materials for DNA functionalization, a systematic surface science study and in particular a side-by-side comparison with GO is critical, which is the main goal of this study.

Materials and Methods

Chemicals. All the DNA samples were purchased from Integrated DNA Technologies (Coralville, IA). The DNA sequences are as follows. T_{15} refers to TTTTTTTTTTTTTTT; FAM-T_{15} refers to labeling a carboxyfluorescein on the 5′-end of T_{15}; FAM-24mer: FAM-ACGCATCTGTGAAGAGAACCTGGG; and c-24mer: CCCAGGTTCTCTTCACAGATGCGT. All the sequences are listed from the 5′ to 3′. Carboxyl GO, monolayer molybdenum disulfide (MoS_2) and tungsten disulfide (WS_2) were from ACS Material (Medford, MA). Sodium chloride, sodium hydroxide, sodium carbonate, sodium bicarbonate, magnesium chloride, adenosine, 4-morpholineethanesulfonate (MES), tris(hydroxymethyl)aminomethane (Tris), and 4-(2-hydroxyethyl) piperazine-1-ethanesulfonate (HEPES) were from Mandel Scientific (Guelph, Ontario, Canada). Dimethyl sulfoxide (DMSO), sodium dodecyl sulfate (SDS), cetyl trimethylammonium bromide (CTAB), Tween 80, and Triton X-100 were from Sigma-Aldrich. Milli-Q water was used for all the experiments.

TEM, UV-vis, and ζ-potential measurement. The MoS_2, WS_2 or GO nanosheets were directly dispersed in Milli-Q water. TEM was performed on a Philips CM10 transmission electron microscope. The sample was prepared by pipetting a drop of the aqueous dispersion (200 µg/mL for MoS_2 and WS_2, 100 µg/mL for GO) onto a 230 mesh copper holy carbon grid and then dried in air. The electronic absorption of MoS_2 and WS_2 (100 µg/mL) and GO (25 µg/mL) was obtained by a UV-vis spectrometer (Agilent 8453A). The ζ-potential (50 µg/mL materials in 10 mM acetate, phosphate or carbonate buffer to cover the full pH range) was measured by dynamic light scattering

on a Malvern Zetasizer Nano ZS90 with a He-Ne laser (633 nm) at 90 degree collecting optics at 25 °C.

DNA adsorption. The kinetics of DNA adsorption was studied by adding different concentrations of MoS_2, WS_2 or GO to 50 μL solution containing 50 nM FAM-labeled DNA in buffer A (20 mM Tris, pH 7.0, 100 mM NaCl, 2 mM $MgCl_2$) at 25 °C. Several different salt concentrations were also tested. The fluorescence was measured on a microplate reader (Infinite F200 Pro, Tecan) with 490 nm excitation and 520 nm emission.

Sensor preparation. A solution of 500 μL containing MoS_2 (2 mg/mL), WS_2 (5 mg/mL) or GO (0.1 mg/mL) was respectively incubated with 500 nM FAM-A_{15} in buffer A in dark at room temperature for 1 h. Then these solutions were washed with buffer A by centrifugation at 15,000 rpm for 10 min. The sensors were finally dispersed in 500 μL buffer A and stored at 4 °C (named solution I, II and III respectively).

DNA desorption. To study DNA desorption induced by chemicals, 5 μL solution I, II or III was respectively centrifuged. After removing the supernatant, the pellets were respectively dispersed in 50 μL of 5 M urea, 10 mM NaOH, 10 mM phosphate, 1 mM adenosine solution, 3 M NaCl, or 50% DMSO. The fluorescence intensity was measured immediately. The background fluorescence was measured by dispersing the same samples in 50 μL buffer A. For surfactant-induced DNA desorption, each well contained 45 μL buffer A and 5 μL solution I, II and III. Then different concentrations of SDS, Tween 80, Triton X-100, or CTAB were added to induce desorption.

DNA sensing. For DNA sensing with MoS_2, WS_2 or GO, each well contained 45 μL buffer A and 5 μL solution I, II or III. Then different concentrations of the cDNA were added to initiate the reaction. Displacement of adsorbed DNA probes was studied using a similar method and a final

of 1 µM of A_{15} or T_{15} DNA without a fluorophore label was added. The FAM-24mer DNA was tested following the same protocol.

Results and Discussion

Materials characterization. Single-layered MoS_2 and WS_2 have a similar structure with the transition metal atoms covered on both sides by sulfur (Figure 1A). Therefore, the chance of DNA interacting directly with the metal centers is quite low except for the edges. While the sulfur atoms are fully exposed, they are not known to interact strongly with DNA. For comparison, GO has a diverse range of oxygen-containing moieties such as hydroxyl, epoxy and carboxyl groups (Figure 1B), allowing hydrogen bonding in addition to pi-pi stacking with DNA.
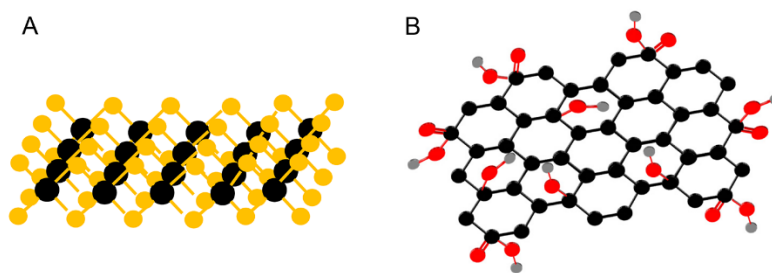

Figure 1. (A) The structure of a single-layered MoS_2 or WS_2. The Mo or W atoms are in black and the sulfur atoms are in yellow. (B) The structure of GO showing rich oxygenated groups: the carbon atoms in black, oxygen in red, and hydrogen in grey.

When dispersed in water at 0.5 mg/mL, MoS_2 is dark green, WS_2 is brown, while GO appears black (inset of Figure 2A). The UV-vis spectra of these samples are shown in Figure 2A. MoS_2 has a peak at ~420 nm and another one at >600 nm, explaining the green color. The absorption features of the other two are less obvious. To characterize their morphology, we performed TEM (Figure 2C-E). Each material appears as large micrometer sized sheets, consistent

6

with their 2D structure. Their similar 2D feature makes it ideal for a side-by-side comparison of their DNA adsorption property.
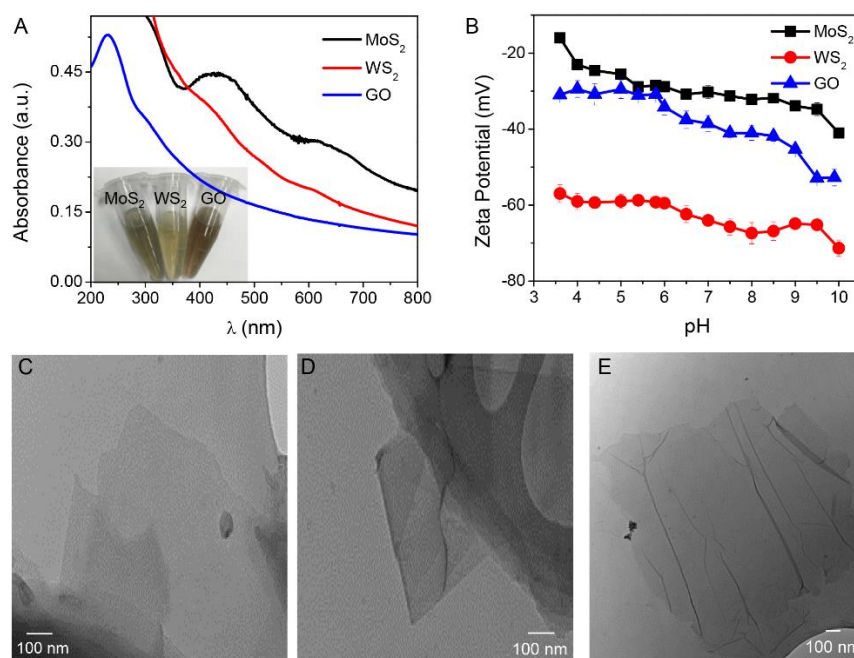

Figure 2. Characterization of these three 2D materials. (A) UV-vis spectra of MoS_2 and WS_2 (100 µg/mL) and GO (25 µg/mL) dispersed in water. Inset: a photograph of these materials (0.5 mg/mL each). (B) Zeta-potential of each material (0.05 mg/mL) as a function of pH in 10 mM buffer (acetate from pH 3.6 to 6; phosphate from pH 6 to 8.5; and carbonate from pH 9 to 10). TEM micrographs of (C) MoS_2, (D) WS_2 and (E) GO.

Since DNA is a highly negatively charged polymer, electrostatic interaction is likely to be important for its adsorption. As such, we measured the zeta-potential of each material as a function of pH (Figure 2B). From pH 3.5 to 10, all these materials are negatively charged. GO has surface carboxyl groups responsible for the negative charges.[14, 38] The negative charges on MoS_2 and WS_2 are attributable to the surface sulfur atoms.[39] Such negative zeta-potentials afford a reasonable

7

colloidal stability in aqueous dispersion. The zeta-potential of WS_2 is much more negative than the other two, and we indeed noticed a better colloidal stability of WS_2 than that of MoS_2.

DNA adsorption. Since DNA adsorption is the first step of interaction, we studied it first. As both DNA and these 2D materials are negatively charged, salt concentration might strongly affect adsorption. Using the FAM-A$_{15}$ DNA, we monitored its background fluorescence for 15 min and then respectively added each material (Figure 3A-C). In the absence of salt, no fluorescence quenching was observed, suggesting the lack of adsorption. With 100 mM NaCl, quenching occurred in all the samples. Further adding 2 mM Mg^{2+} resulted in even faster and stronger quenching in each case. Our results are consistent with that salt is required to overcome electrostatic repulsion for DNA adsorption. In addition, all these materials can quench fluorescence, which is useful for analytical applications.[20, 21, 40]

We also noticed that at the same materials and salt concentration, GO induced the highest amount of quenching. To quantitatively understand this, we fixed the DNA and salt concentration, and monitored fluorescence quenching as a function of materials concentration (Figure 3D-F). In each case, a higher concentration induced more significant fluorescence quenching. With 20 µg/mL of GO, full adsorption was achieved, while it takes much more of MoS_2 and WS_2. We plotted the relative fluorescence quenching as a function of materials concentration (Figure 3G). At low concentration, a linear fluorescence quenching was observed. We attribute this mainly to adsorption, and the amount of fluorescence drop due to light scattering/absorption by these materials was neglected. The slopes of these curves represent the adsorption capacity at the experimental condition. We calculated that the capacity of GO is 36.6 times higher than that of MoS_2, and 33.0 times higher of WS_2.
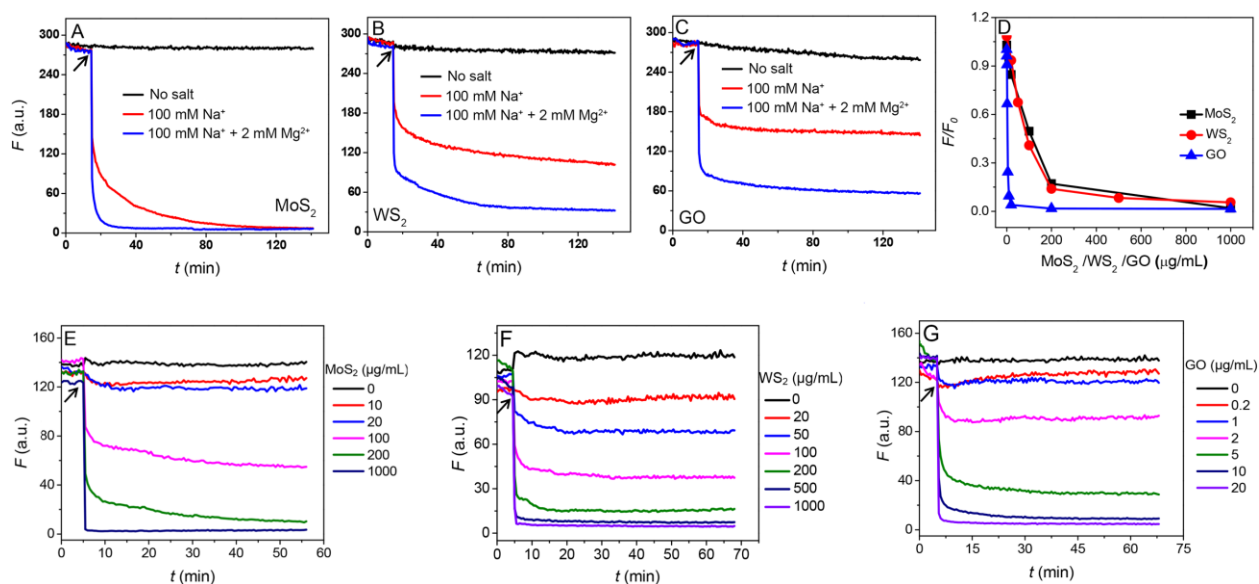
Figure 3. Kinetics of FAM-labeled A_{15} (50 nM) adsorption by (A) MoS_2 (200 µg/mL), (B) WS_2 (500 µg/mL) and (C) GO (10 µg/mL) at three different salt concentrations. The materials were added at 15 min indicated by the arrowhead. (D) Relative fluorescence quenching as a function of materials concentration. The initial slope indicates the relative adsorption capacity. Kinetics of the DNA (50 nM) adsorption by various concentrations of (E) MoS_2, (F) WS_2 and (G) GO in buffer (100 mM NaCl, 2 mM Mg^{2+}, 20 mM Tris, pH 7.0).

GO has a much lower molecular weight (made mainly of carbon and oxygen). With the same mass concentration, GO has a larger geometric surface area. The theoretical surface area is 2630 m^2/g for a single graphene sheet. With oxygenated groups present, the surface area of GO is smaller than the theoretical graphene value. The oxygen content of our GO is about 40%,[14] leading to a theoretical specific surface area of ~1575 m^2/g. The surface area of the dichalcogenides are smaller since they contain heavier atoms. MoS_2 can reach 210 m^2/g,[41] and WS_2 is around 100 m^2/g.[42] This difference in specific surface area can account for a large fraction of the difference in DNA adsorption capacity. In addition, GO might have a higher adsorption affinity, allowing more

9

DNA to be adsorbed. For example, only GO can form pi-pi stacking and strong hydrogen bonding, while the other two materials cannot. The adsorption affinity might account for the rest of difference in adsorption capacity, and this is the topic of the subsequent section.

DNA desorption. To compare adsorption affinity and to understand the mechanism of DNA adsorption, we next studied DNA desorption. For this purpose, a FAM-labeled DNA was pre-adsorbed to prepare an adsorption complex with a low fluorescence. We monitored its background for a few minutes to ensure stable adsorption. Then a DNA denaturing agent was added to induce DNA desorption and the kinetics of fluorescence enhancement was followed. For each sample, we compared the fluorescence intensity with the free DNA in the buffer but without adding nanomaterials to calculate the desorption percentage. Each denaturing agent was used to probe a type of intermolecular force.

It is known that hydrogen bonding plays an important role in DNA adsorption by GO, which was supported by urea washing.[43] Following this, we exposed these three adsorption complexes to 5 M urea (Figure 4A). We observed a significant release of DNA from GO (>50%) but much less from the other two materials. This suggests that DNA adsorption by MoS_2 and WS_2 is independent of hydrogen bonding. This is reasonable since no hydrogen bond donors are on these materials and the ability of sulfur to be a hydrogen bond acceptor is much weaker than oxygen due to the low electronegativity of sulfur.

Next, the effect of pH was studied (Figure 4B). In this case, a final of 10 mM NaOH was added to each sample to raise the pH. Fluorescence enhancement was observed in all the samples, and GO had the highest fluorescence increase and thus the most DNA desorption. In general, at higher pH, the surface of these materials becomes more negative (Figure 2B). This would increase the electrostatic repulsion with DNA and weakening adsorption. Hydrogen bonding can also be

disrupted at high pH due to deprotonation of hydrogen bond donors, which may explain the more desorption from GO. We did not try acidic pH since low pH would increase the adsorption affinity,[44] and thus no desorption is expected.
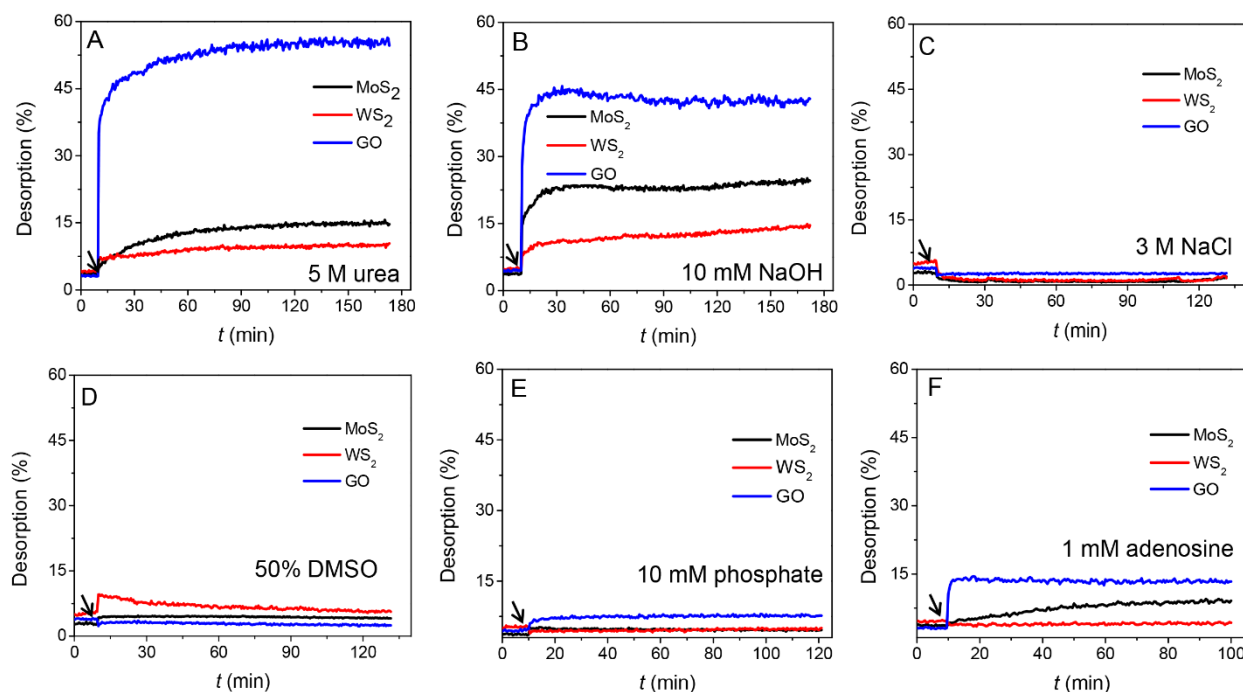

Figure 4. Comparison of DNA desorption from MoS_2, WS_2 and GO under various denaturing conditions. Kinetics of DNA desorption from MoS_2, WS_2 and GO after adding (A) 5 M urea, (B) 10 mM NaOH, (C) 3 M NaCl, (D) 50% DMSO, (E) 10 mM phosphate, and (F) 1 mM adenosine, The materials were added at 10 min indicated by the arrowhead.

Although electrostatic attraction is unlikely to take place between DNA and these materials, we still screened the charge interaction by adding 3 M NaCl. Indeed, we observed enhanced adsorption since the fluorescence slightly dropped for all the samples (Figure 4C). We next probed hydrophobic interactions by adding an organic solvent, DMSO, which can dissolve hydrophobic

molecules (Figure 4D). In this case, we also failed to see fluorescence enhancement for any material suggesting that hydrophobic interactions is insignificant for DNA adsorption.

DNA is made of nucleosides and a phosphate backbone, and DNA is known to use these chemical groups to interact with various materials. For example, DNA uses its phosphate to adsorb onto many metal oxides,[45] while uses its base coordination to bind to gold nanoparticles.[46] To probe possible chemical interactions, we next challenged the samples with 10 mM free inorganic phosphate or 1 mM adenosine. With phosphate, none of them showed much desorption, suggesting that the DNA does not use its phosphate backbone for adsorption. This is consistent with that the metal centers in the dichalcogenides are shielded. On the other hand, we observed a lot more desorption from GO upon adding adenosine. This is consistent with the fact that DNA is adsorbed on GO using its nucleobases (hydrogen bonding and pi-pi stacking).[47] The two dichalcogenides, however, failed to show much response to adenosine either, especially for WS_2.

Taken together, the above studies have ruled out hydrogen bonding, electrostatic attraction, hydrophobic interactions, and chemical interactions for MoS_2 and WS_2 to interact with DNA. As such, we reason that they adsorb DNA mainly via vdW force, which is a ubiquitous intermolecular/surface force. Using first principle density function theory (DFT), Vovusha and Sanyal indicated that all the four nucleobases interact with MoS_2 and WS_2 via vdW force, which is consistent with our conclusion.[35] They predicted that for individual nucleobases, the affinity on MoS_2 and WS_2 follows the order of G > A > T > C with atomic level details. For example, the H atom of the CH_3 group in adenine interacts with the S atom of the surface. For cytosine, the H of the CH_3 group and the O atom are relatively closer to the substrates. In another theoretical study, the vdW force was also deemed critical and order of interaction was determined to be G > A/C > T.[34] The fact that guanine adsorbs very tightly is also consistent with our observation in this study

(*vide infra*). MoS_2 and WS_2 sheets stack to form bulk materials via vdW force. The relatively large electronegativity between Mo/W and S can resulted in polarized electron distribution, which is favorable for vdW interactions (e.g. dipole and induced dipole interactions). Therefore, it is not surprising that these two materials mainly use vdW force for adsorbing DNA.

Our results above also suggest that the vdW force between DNA and GO is weaker than that between DNA and the dichalcogenides. For example, when urea was added to disrupt hydrogen bonding, much more DNA desorbed from GO. In the presence of urea, GO should still be able to interact with DNA via vdW force. As such, GO has much weaker vdW interactions with DNA.

DNA displacement by surfactants. After studying the force responsible for DNA adsorption by adding various denaturing agents, we next examined DNA displacement by other molecules. Such molecules do not denature DNA but they compete with DNA for the surface adsorption sites, which may further increase our fundamental understanding. First, we added various surfactants to displace adsorbed DNA. SDS is a small molecule anionic surfactant. While it had no effect on GO, ~10% DNA desorbed from the other two surfaces (Figure 5A). A slightly different trend was observed CTAB, where desorption was observed only from MoS_2 (Figure 5B). With ten times higher CTAB (i.e. 0.1%), DNA also desorbed from WS_2, but still not from GO (Figure S1). Therefore, regardless of the charge of these small molecule surfactants, they both induced more desorption from the dichalcogenides.

We further tested two larger surfactant molecules: Tween 80 (Figure 5C) and Triton X-100 (Figure 5D). In both cases, the highest desorption occurred with MoS_2 and the least with GO, leaving WS_2 in between. This is consistent with that the surfactants interact with the dichalcogenides via their hydrophobic tails using vdW force to displace DNA. As such, the charge

on the surfactant headgroups is less important.[48] This is in direct competition with the adsorbed DNA since the same force was involved. On the other hand, GO adsorption is based on other forces and is thus less affected. It is also interesting to note that the higher molecular weight Tween 80 and Triton X-100 desorbed more DNA than the small molecule surfactants SDS and CTAB. This is likely due to the higher molecular weight surfactants (both are non-charged) having a stronger vdW force with the surfaces. The fact that DNA is adsorbed more tightly on GO when probed by surfactants, but less tightly on GO when probed by the denaturing agents also supports the importance of the vdW force on the dichalcogenides.
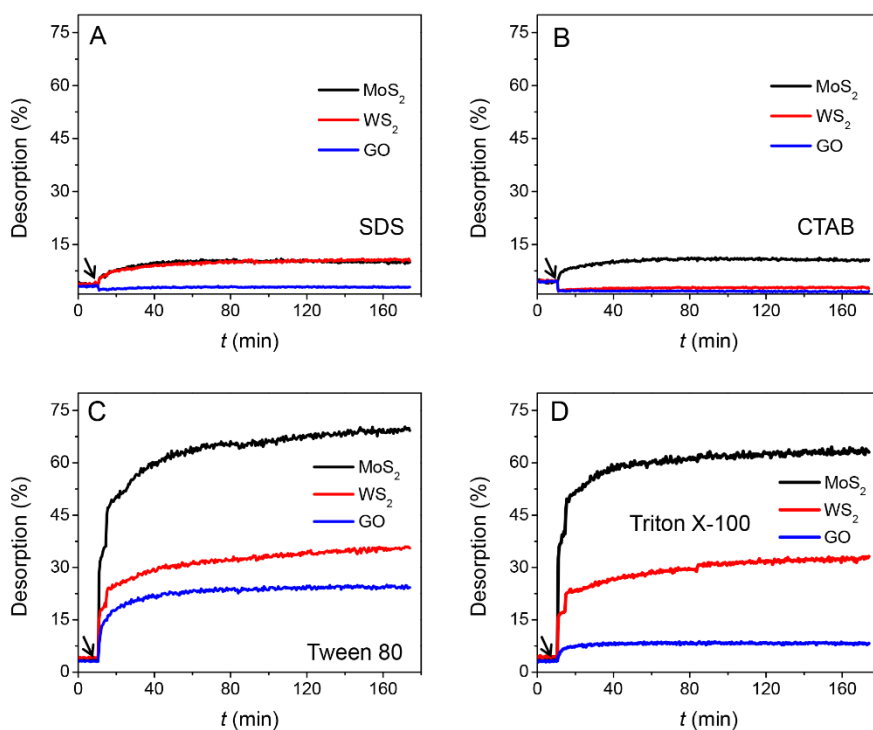

Figure 5. Kinetics of FAM-A_{15} DNA desorption from MoS_2, WS_2 and GO after adding 0.01% (A) SDS, (B) CTAB, (C) Tween 80, and (D) Triton X-100. The reaction buffer contained 20 mM Tris, pH 7.0, 100 mM NaCl, and 2 mM $MgCl_2$. The surfactants were added at 10 min as indicated by the arrowheads.

14

Effect of DNA sequence and length. Since DNA adsorption by GO has been extensively studied,[11-15] this work is focused on MoS_2 and WS_2. Considering the similarity between MoS_2 and WS_2, we chose the latter to study the effect of DNA sequence and length. The four 15-mer FAM-labeled DNA homopolymers were respectively adsorbed on WS_2, and then Tween 80 was added to induce desorption. We observed the most desorption with C_{15} followed by T_{15}, A_{15} and G_{15} (Figure 6A). Therefore, adsorption of the purines are stronger than the pyrimidines. This is consistent with the previous theoretical calculations of vdW force based DNA base adsorption.[34, 35] Similarly, the effect of DNA length was studied using poly-A DNA. Interestingly, while longer DNA showed less desorption, the difference was quite small (Figure 6B). It might be that each DNA did not use all its bases to adsorb and the advantage of longer DNA is less obvious. For example, it has been simulated on graphene that ssDNA has two competing forces on the surface: inter-nucleobase stacking and nucleobase stacking with graphene.[49] The former force results in that only a fraction of the bases are adsorbed. A similar situation is likely to also occur on the dichalcogenide surfaces.
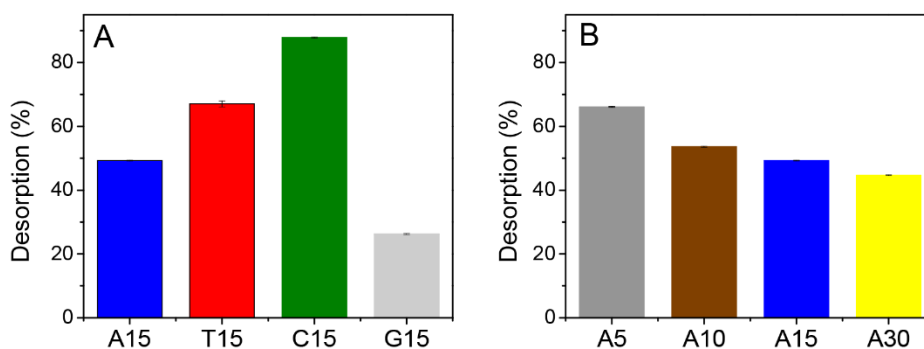

Figure 6. Effect of DNA sequence and length on DNA adsorption affinity on WS_2. Fluorescence measurement of (A) different sequences and (B) different lengths of FAM-labeled DNA desorption from WS_2 after 20 min incubation with 0.01% Tween 80. The reaction buffer contained 20 mM Tris, pH 7.0 with 100 mM NaCl and 2 mM $MgCl_2$.

DNA displacement by DNA. Since DNA is only physisorbed in this work, they can be displaced by other molecules, such as the surfactants demonstrated above. For DNA sensing applications, an interesting question is non-specific DNA displacement by DNA. To study this, we adsorbed FAM-A$_{15}$ and then added its cDNA, T$_{15}$ or the same A$_{15}$ DNA but without the fluorophore label. For MoS$_2$ and WS$_2$, we observed more fluorescence signal when T$_{15}$ was added, suggesting that DNA hybridization plays a key role here. Non-specific displacement by A$_{15}$ also occurred, but to a smaller extent. However, more displacement by A$_{15}$ occurred on GO than hybridization by T$_{15}$, which is consistent with our previous observation.[50] This is an important difference, and suggests that A$_{15}$ adsorption by GO might be more favorable than its hybridization with T$_{15}$. On the other hand, DNA adsorption by the dichalcogenide surfaces is weaker to allow DNA specific hybridization to be the dominating interaction.
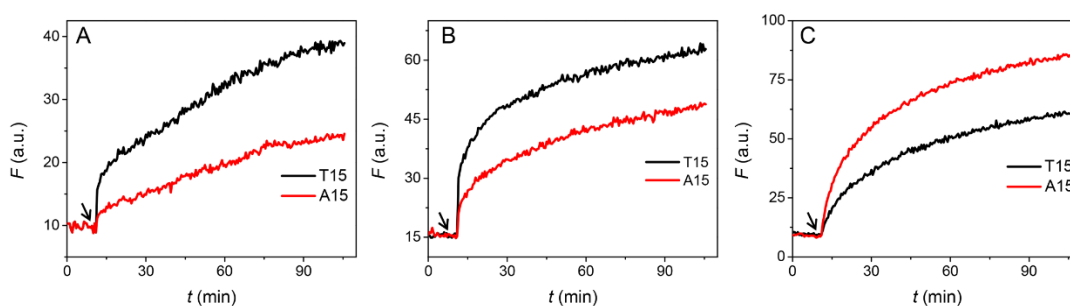

Figure 7. DNA hybridization and displacement. The FAM-A$_{15}$ DNA probe was first adsorbed by each surface and then a non-labeled T$_{15}$ or A$_{15}$ DNA was added to induce probe desorption from (A) MoS$_2$, (B) WS$_2$, and (C) GO. The DNA was added at 10 min indicated by the arrowheads.

DNA sensing with a random sequence. After these fundamental surface science studies, we next compared the analytical performance of these materials for DNA detection. Our sensing scheme is shown in Figure 8A. A fluorescent probe DNA was first adsorbed and its cDNA was added to

induced signaling.[27] The above studies in Figure 7 used two model DNA homopolymer sequences for mechanistic studies. Here we employed a random sequence for testing analytical performance. The kinetics of signaling on each surface are shown in Figure 8B-D, respectively. They all showed cDNA concentration dependent fluorescence enhancement, thus supporting potential sensing applications. We quantified the relative fluorescence enhancement at 10 min after adding the cDNA (Figure 8E). The GO sample showed the strongest signal enhancement reaching ~18-fold, while the other two had a similar performance of ~4-fold. A similar trend was observed when a different probe DNA sequence was used (Figure S2). The slope of the initial linear increase was compared (Figure 8F), and the GO sample is 4.3-fold more sensitivity (note this slope is the sensitivity of the sensors). We also calculated the detection limits of these sensors based on the signal greater than 3 times of background variation, and they turned out to have a similar detection limit (Figure 8G). This is likely due to a less fluctuated background to compensate for the lower sensitivity of the dichalcogenates. While cDNA-concentration-dependent response has been demonstrated, such sensors may suffer from non-specific displacement by other molecules and thus produce false positive signals. Therefore, careful controls and internal references are needed to ensure correct analytical interpretations. For example, by co-adsorbing a random DNA labeled with a different fluorophore as an internal standard, it is possible to identify false positive signals due to non-specific probe displacement.[51] Covalent linking is another strategy,[52] which however has yet to be developed for the dichalcogenates.
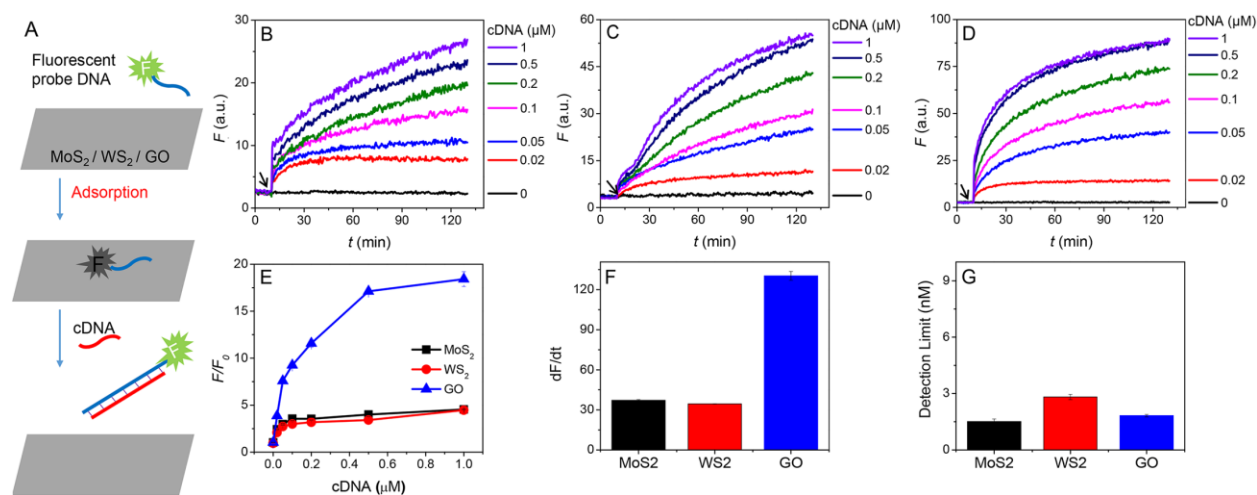
Figure 8. Schematics of DNA sensing using a fluorophore-labeled DNA probe. The probe is adsorbed by MoS_2, WS_2 or GO, resulting in fluorescence quenching. After adding the target cDNA, fluorescence is recovered due to DNA hybridization. Kinetics of probe desorption from (B) MoS_2, (C) WS_2 and (D) GO in the presence of various concentrations of cDNA. The arrowheads indicate the time point when cDNA was added (10 min). (E) The relative fluorescence enhancements of MoS_2, WS_2 and GO after 10 min reaction. (F) The slope of the initial linear signal increase in (B-D) indicative of sensor sensitivity. (G) The detection limits of the three sensors from (B-D).

Conclusions

In summary, we compared DNA adsorption and desorption from three representative 2D materials: GO, MoS_2 and WS_2. In particular, fundamental surface forces were probed by various chemicals, and the implication for DNA sensing was emphasized. We measured the zeta-potential of each material and they were all negatively charged. As a result, DNA adsorption requires a high ionic strength to screen charge repulsion. While GO, MoS_2 and WS_2 can all adsorb DNA and quench the fluorescence of the absorbed fluorophore, the mechanism of DNA adsorption on each material

is quite different. DNA is adsorbed on GO mainly via pi-pi stacking and hydrogen bonding, while MoS_2 and WS_2 rely on vdW force as probed by various denaturing conditions. Denaturing agents such as urea and strong base induced more DNA desorption from GO, while all the tested surfactants are more effective to displace DNA from the two dichacolgenides. Using FAM-A_{15} as a probe, T_{15} induced more probe desorption than A_{15} on MoS_2 and WS_2, suggesting specific DNA hybridization. The opposite however was observed on GO, suggesting non-specific displacement. When their performance for DNA detection is compared, the GO surface had the highest sensitivity, while the detection limit of the three sensors turned out to be similar. These fundamental understandings are valuable for designing and optimization of sensors and devices based on DNA and 2D materials.

Supporting Information Available

This information is available free of charge via the Internet at http://pubs.acs.org/.

DNA desorption by high concentration of surfactants and additional DNA sensing data (PDF).

References

(1)   Yang, K.; Feng, L.; Shi, X.; Liu, Z., Nano-Graphene in Biomedicine: Theranostic Applications. *Chem. Soc. Rev.* **2013**, 42, 530-547.

(2)   Jones, M. R.; Seeman, N. C.; Mirkin, C. A., Programmable Materials and the Nature of the DNA Bond. *Science* **2015**, 347, 1260901.

(3)   Tan, L. H.; Xing, H.; Lu, Y., DNA as a Powerful Tool for Morphology Control, Spatial Positioning, and Dynamic Assembly of Nanoparticles. *Acc. Chem. Res.* **2014**, 47, 1881-1890.

(4)   Wang, H.; Yang, R. H.; Yang, L.; Tan, W. H., Nucleic Acid Conjugated Nanomaterials for Enhanced Molecular Recognition. *ACS Nano* **2009**, 3, 2451-2460.

(5)   Liu, J.; Cao, Z.; Lu, Y., Functional Nucleic Acid Sensors. *Chem. Rev.* **2009**, 109, 1948–1998.

(6)   Song, S. P.; Qin, Y.; He, Y.; Huang, Q.; Fan, C. H.; Chen, H. Y., Functional Nanoprobes for Ultrasensitive Detection of Biomolecules. *Chem. Soc. Rev.* **2010**, 39, 4234-4243.

(7)   Novoselov, K. S.; Falko, V. I.; Colombo, L.; Gellert, P. R.; Schwab, M. G.; Kim, K., A Roadmap for Graphene. *Nature* **2012**, 490, 192-200.

(8)   Chen, D.; Feng, H.; Li, J., Graphene Oxide: Preparation, Functionalization, and Electrochemical Applications. *Chem. Rev.* **2012**, 112, 6027-6053.

(9)   Liu, Z.; Liu, B.; Ding, J.; Liu, J., Fluorescent Sensors Using DNA-Functionalized Graphene Oxide. *Anal. Bioanal. Chem.* **2014**, 406, 6885-6902.

(10)   Lu, C. H.; Yang, H. H.; Zhu, C. L.; Chen, X.; Chen, G. N., A Graphene Platform for Sensing Biomolecules. *Angew. Chem. Int. Ed.* **2009**, 48, 4785-4787.

(11)   Liu, B.; Salgado, S.; Maheshwari, V.; Liu, J., DNA Adsorbed on Graphene and Graphene Oxide: Fundamental Interactions, Desorption and Applications. *Curr. Opin. Colloid Interface Sci.* **2016**, 26, 41-49.

(12)   Wu, M.; Kempaiah, R.; Huang, P.-J. J.; Maheshwari, V.; Liu, J., Adsorption and Desorption of DNA on Graphene Oxide Studied by Fluorescently Labeled Oligonucleotides. *Langmuir* **2011**, 27, 2731–2738.

(13)   Park, J. S.; Goo, N.-I.; Kim, D.-E., Mechanism of DNA Adsorption and Desorption on Graphene Oxide. *Langmuir* **2014**, 30, 12587-12595.

(14)   Lu, C.; Huang, P.-J. J.; Liu, B.; Ying, Y.; Liu, J., Comparison of Graphene Oxide and Reduced Graphene Oxide for DNA Adsorption and Sensing. *Langmuir* **2016**, 32, 10776–10783.

(15)   Lee, J.; Yim, Y.; Kim, S.; Choi, M.-H.; Choi, B.-S.; Lee, Y.; Min, D.-H., In-Depth Investigation of the Interaction between DNA and Nano-Sized Graphene Oxide. *Carbon* **2016**, 97, 92-98.

(16)   Chhowalla, M.; Shin, H. S.; Eda, G.; Li, L. J.; Loh, K. P.; Zhang, H., The Chemistry of Two-Dimensional Layered Transition Metal Dichalcogenide Nanosheets. *Nat. Chem.* **2013**, 5, 263-275.

(17)   Butler, S. Z.; Hollen, S. M.; Cao, L.; Cui, Y.; Gupta, J. A.; Gutiérrez, H. R.; Heinz, T. F.; Hong, S. S.; Huang, J.; Ismach, A. F.; Johnston-Halperin, E.; Kuno, M.; Plashnitsa, V. V.; Robinson, R. D.; Ruoff, R. S.; Salahuddin, S.; Shan, J.; Shi, L.; Spencer, M. G.; Terrones, M.; Windl, W.; Goldberger, J. E., Progress, Challenges, and Opportunities in Two-Dimensional Materials Beyond Graphene. *ACS Nano* **2013**, 7, 2898-2926.

(18)   Xu, M.; Liang, T.; Shi, M.; Chen, H., Graphene-Like Two-Dimensional Materials. *Chem. Rev.* **2013**, 113, 3766-3798.

(19)   Li, B. L.; Wang, J.; Zou, H. L.; Garaj, S.; Lim, C. T.; Xie, J.; Li, N. B.; Leong, D. T., Low-Dimensional Transition Metal Dichalcogenide Nanostructures Based Sensors. *Adv. Funct. Mater.* **2016**, 26, 7034-7056.

(20)   Xi, Q.; Zhou, D.-M.; Kan, Y.-Y.; Ge, J.; Wu, Z.-K.; Yu, R.-Q.; Jiang, J.-H., Highly Sensitive and Selective Strategy for Microrna Detection Based on WS_2 Nanosheet Mediated Fluorescence Quenching and Duplex-Specific Nuclease Signal Amplification. *Anal. Chem.* **2014**.

(21)   Huang, J.; Ye, L.; Gao, X.; Li, H.; Xu, J.; Li, Z., Molybdenum Disulfide-Based Amplified Fluorescence DNA Detection Using Hybridization Chain Reactions. *J. Mater. Chem. B* **2015**, 3, 2395-2401.

(22)   Zhu, C.; Zeng, Z.; Li, H.; Li, F.; Fan, C.; Zhang, H., Single-Layer Mos2-Based Nanoprobes for Homogeneous Detection of Biomolecules. *J. Am. Chem. Soc.* **2013**, 135, 5998-6001.

(23)   Loan, P. T. K.; Zhang, W.; Lin, C.-T.; Wei, K.-H.; Li, L.-J.; Chen, C.-H., Graphene/MoS_2 Heterostructures for Ultrasensitive Detection of DNA Hybridisation. *Adv. Mater.* **2014**, 26, 4838-4844.

(24)   Farimani, A. B.; Min, K.; Aluru, N. R., DNA Base Detection Using a Single-Layer MoS_2. *ACS Nano* **2014**, 8, 7914-7922.

(25)   Wang, T.; Zhu, R.; Zhuo, J.; Zhu, Z.; Shao, Y.; Li, M., Direct Detection of DNA Below ppb Level Based on Thionin-Functionalized Layered MoS_2 Electrochemical Sensors. *Anal. Chem.* **2014**, 86, 12064-12069.

(26)   Zhang, Y.; Zheng, B.; Zhu, C.; Zhang, X.; Tan, C.; Li, H.; Chen, B.; Yang, J.; Chen, J.; Huang, Y.; Wang, L.; Zhang, H., Single-Layer Transition Metal Dichalcogenide Nanosheet-Based Nanosensors for Rapid, Sensitive, and Multiplexed Detection of DNA. *Adv. Mater.* **2015**, 27, 935-939.

(27)   Yuan, Y.; Li, R.; Liu, Z., Establishing Water-Soluble Layered WS_2 Nanosheet as a Platform for Biosensing. *Anal. Chem.* **2014**, 86, 3610-3615.

(28)   Ge, J.; Ou, E.-C.; Yu, R.-Q.; Chu, X., A Novel Aptameric Nanobiosensor Based on the Self-Assembled DNA-MoS_2 Nanosheet Architecture for Biomolecule Detection. *J. Mater. Chem. B* **2014**, 2, 625-628.

(29)   Kong, R.-M.; Ding, L.; Wang, Z.; You, J.; Qu, F., A Novel Aptamer-Functionalized MoS_2 Nanosheet Fluorescent Biosensor for Sensitive Detection of Prostate Specific Antigen. *Anal. Bioanal. Chem.* **2015**, 407, 369-377.

(30)   Zhang, H.; Ruan, Y.; Lin, L.; Lin, M.; Zeng, X.; Xi, Z.; Fu, F., A Turn-Off Fluorescent Biosensor for the Rapid and Sensitive Detection of Uranyl Ion Based on Molybdenum Disulfide Nanosheets and Specific DNAzyme. *Spectrochimica Acta A:* **2015**, 146, 1-6.

(31)   Jin, K.; Xie, L.; Tian, Y.; Liu, D., Au-Modified Monolayer MoS_2 Sensor for DNA Detection. *J. Phys. Chem. C* **2016**, 120, 11204-11209.

(32)   Li, B. L.; Zou, H. L.; Lu, L.; Yang, Y.; Lei, J. L.; Luo, H. Q.; Li, N. B., Size-Dependent Optical Absorption of Layered MoS_2 and DNA Oligonucleotides Induced Dispersion Behavior for Label-Free Detection of Single-Nucleotide Polymorphism. *Adv. Funct. Mater.* **2015**, 25, 3541-3550.

(33)   Bang, G. S.; Cho, S.; Son, N.; Shim, G. W.; Cho, B.-K.; Choi, S.-Y., DNA-Assisted Exfoliation of Tungsten Dichalcogenides and Their Antibacterial Effect. *ACS Appl. Mater. Inter.* **2016**, 8, 1943-1950.

(34)   Sharma, M.; Kumar, A.; Ahluwalia, P. K., Optical Fingerprints and Electron Transport Properties of DNA Bases Adsorbed on Monolayer MoS_2. *RSC Adv.* **2016**, 6, 60223-60230.

(35)   Vovusha, H.; Sanyal, B., Adsorption of Nucleobases on 2D Transition-Metal Dichalcogenides and Graphene Sheet: A First Principles Density Functional Theory Study. *RSC Adv.* **2015**, 5, 67427-67434.

(36)   Balcioglu, M.; Rana, M.; Robertson, N.; Yigit, M. V., DNA-Length-Dependent Quenching of Fluorescently Labeled Iron Oxide Nanoparticles with Gold, Graphene Oxide and MoS_2 Nanostructures. *ACS Appl. Mater. Inter.* **2014**, 6, 12100-12110.

(37)   He, S. J.; Song, B.; Li, D.; Zhu, C. F.; Qi, W. P.; Wen, Y. Q.; Wang, L. H.; Song, S. P.; Fang, H. P.; Fan, C. H., A Graphene Nanoprobe for Rapid, Sensitive, and Multicolor Fluorescent DNA Analysis. *Adv. Funct. Mater.* **2010**, 20, 453-459.

(38)   Cote, L. J.; Kim, J.; Zhang, Z.; Sun, C.; Huang, J. X., Tunable Assembly of Graphene Oxide Surfactant Sheets: Wrinkles, Overlaps and Impacts on Thin Film Properties. *Soft Matter* **2010**, 6, 6096-6101.

(39)   Sun, L.; Huang, H.; Peng, X., Laminar MoS_2 Membranes for Molecule Separation. *Chem. Commun.* **2013**, 49, 10718-10720.

(40)   Loo, A. H.; Bonanni, A.; Pumera, M., Strong Dependence of Fluorescence Quenching on the Transition Metal in Layered Transition Metal Dichalcogenide Nanoflakes for Nucleic Acid Detection. *Analyst* **2016**, 141, 4654-4658.

(41)   Afanasiev, P.; Xia, G.-F.; Berhault, G.; Jouguet, B.; Lacroix, M., Surfactant-Assisted Synthesis of Highly Dispersed Molybdenum Sulfide. *Chem. Mater.* **1999**, 11, 3216-3219.

(42)   Shi, Y.; Wan, Y.; Liu, R.; Tu, B.; Zhao, D., Synthesis of Highly Ordered Mesoporous Crystalline WS_2 and MoS_2 via a High-Temperature Reductive Sulfuration Route. *J. Am. Chem. Soc.* **2007**, 129, 9522-9531.

(43)   Park, J. S.; Na, H.-K.; Min, D.-H.; Kim, D.-E., Desorption of Single-Stranded Nucleic Acids from Graphene Oxide by Disruption of Hydrogen Bonding. *Analyst* **2013**, 138, 1745-1749.

(44)   Huang, P.-J. J.; Kempaiah, R.; Liu, J., Synergistic pH Effect for Reversible Shuttling Aptamer-Based Biosensors between Graphene Oxide and Target Molecules. *J. Mater. Chem.* **2011**, 21, 8991-8993.

(45)   Liu, B.; Liu, J., Comprehensive Screen of Metal Oxide Nanoparticles for DNA Adsorption, Fluorescence Quenching, and Anion Discrimination. *ACS Appl. Mater. Inter.* **2015**, 7, 24833-24838.

(46)   Kimura-Suda, H.; Petrovykh, D. Y.; Tarlov, M. J.; Whitman, L. J., Base-Dependent Competitive Adsorption of Single-Stranded DNA on Gold. *J. Am. Chem. Soc.* **2003**, 125, 9014-9015.

(47)   Liu, J., Adsorption of DNA onto Gold Nanoparticles and Graphene Oxide: Surface Science and Applications. *Phys. Chem. Chem. Phys.* **2012**, 14, 10485-10496.

(48)   Gupta, A.; Arunachalam, V.; Vasudevan, S., Water Dispersible, Positively and Negatively Charged MoS_2 Nanosheets: Surface Chemistry and the Role of Surfactant Binding. *J. Phys. Chem. Lett.* **2015**, 6, 739-744.

(49)   Manna, A. K.; Pati, S. K., Theoretical Understanding of Single-Stranded DNA Assisted Dispersion of Graphene. *J. Mater. Chem. B* **2013**, 1, 91-100.

(50)   Liu, B.; Sun, Z.; Zhang, X.; Liu, J., Mechanisms of DNA Sensing on Graphene Oxide. *Anal. Chem.* **2013**, 85, 7987-7993.

(51)   Tan, X.; Chen, T.; Xiong, X.; Mao, Y.; Zhu, G.; Yasun, E.; Li, C.; Zhu, Z.; Tan, W., Semiquantification of ATP in Live Cells Using Nonspecific Desorption of DNA from Graphene Oxide as the Internal Reference. *Anal. Chem.* **2012**, 84, 8622-8627.

(52)   Huang, P.-J. J.; Liu, J., A Molecular Beacon Lighting up on Graphene Oxide. *Anal. Chem.* **2012**, 84, 4192-4198.